Explosion triggering by an accelerating flame

Vitaly Bychkov[1] and V'yacheslav Akkerman[1,2]
[1]*Institute of Physics, Umeå University, SE-901 87 Umeå, Sweden*
[2]*Nuclear Safety Institute (IBRAE) of Russian Academy of Sciences, B. Tulskaya 52, 115191 Moscow, Russia*
(Received 14 October 2005; revised manuscript received 9 February 2006; published 19 June 2006)

The analytical theory of explosion triggering by an accelerating flame is developed. The theory describes the structure of a one-dimensional isentropic compression wave pushed by the flame front. The condition of explosion in the gas mixture ahead of the flame front is derived; the instant of the explosion is determined provided that a mechanism of chemical kinetics is known. As an example, it is demonstrated how the problem is solved in the case of a single reaction of Arrhenius type, controlling combustion both inside the flame front and ahead of the flame. The model of an Arrhenius reaction with a cutoff temperature is also considered. The limitations of the theory due to the shock formation in the compression wave are found. Comparison of the theoretical results to the previous numerical simulations shows good agreement.

DOI: 10.1103/PhysRevE.73.066305 PACS number(s): 47.15.−x, 47.40.−x, 82.33.Vx

I. INTRODUCTION

A front of exothermal chemical reactions (combustion) may propagate in two different hydrodynamic regimes: one of them is the subsonic regime of flame, the other one is the supersonic regime of detonation [1–3]. In a flame the cold fuel mixture ahead of the front is heated by thermal conduction, which initiates the reaction in the cold gas. In the case of detonation the reaction is triggered by a leading shock wave, which compresses and heats the cold fuel mixture. The flame and the detonation have quite different properties for the same fuel mixture; particularly, the propagation velocity of the reaction front may differ by several orders of magnitude in these two regimes. Still, it was observed in many experiments that a flame front in a tube may spontaneously accelerate and trigger detonation: the phenomenon is known as the deflagration-to-detonation transition (DDT) [2–8]. The first explanation of the DDT goes back to the classical work by Shelkin [5]. According to this explanation, a flame front interacts with the tube walls due to the nonslip boundary conditions at the walls and the thermal expansion of the burning matter. This interaction makes the flame front curved, and the flame accelerates. The accelerating flame acts like a piston pushing compression waves into the fuel mixture. The compression waves heat the cold gas and reduce the reaction time in the mixture ahead of the flame front. Finally, the fuel mixture explodes ahead of the flame, and the explosion develops into detonation. Though this qualitative description of the DDT was generally accepted since the 1940s, still, there was much trouble in developing the qualitative description into a quantitative theory. On the contrary, the DDT was considered as one of the most difficult problems of combustion science. The main reason for that was a common belief that the flame acceleration and the DDT are possible only for strongly turbulent flames in agreement with the experimental observations [2–8]. However, the theory of turbulent burning by itself is a superproblem of combustion science waiting for solution in spite of almost a century of intensive research, see, for example, Refs. [2,9–22].

Only recently, an idea was suggested that the flame acceleration and the DDT may happen even for laminar flames in a tube with adiabatic walls and with one end closed [23,24]. Though it is difficult to obtain adiabatic walls in a real experiment, such a situation is quite common in numerical simulations. Unlike real experiments, in numerical simulations it is much easier to control the boundary and the initial conditions. In that way, it becomes possible to separate the mechanism of principal importance for the flame acceleration from other supplementary effects, which is quite difficult to achieve in reality. Particularly, the possibility of the DDT in the scope of a laminar flow was illustrated by a direct simulation run in Ref. [23] starting from an accelerating flame and up to the well-developed detonation. The idea of a laminar DDT turned out to be incredibly productive for the theory, since it allows avoiding the difficulties related to turbulence. Based on this idea, the analytical theory of laminar accelerating flames in tubes with adiabatic walls was developed in a recent paper [25]; the theory was validated by extensive direct numerical simulations. It was obtained that asymptotically in time a flame front accelerates exponentially as

$$U_w = U_f \exp\left(\sigma \frac{U_f t}{R}\right), \tag{1}$$

where U_f is the planar flame velocity, U_w is the velocity of the flame propagation proportional to the total surface area of the flame front, R is the tube half width (radius), and the dimensionless acceleration rate σ depends on the flow parameters. In Ref. [25] the acceleration rate was found analytically for the case of a two-dimensional (2D) channel flow as

$$\sigma = \frac{(\mathrm{Re}-1)^2}{4\,\mathrm{Re}}\left(\sqrt{1+\frac{4\,\mathrm{Re}\,\Theta}{(\mathrm{Re}-1)^2}}-1\right)^2, \tag{2}$$

where $\mathrm{Re}=U_f R/\nu$ is the Reynolds number (ν is the kinematical viscosity of the fuel mixture) and $\Theta=\rho_f/\rho_b$ is the expansion coefficient, which shows density variations of the burning matter from the fuel mixture ρ_f to the burnt gas ρ_b. The analytical formula for σ is in good agreement with numerical simulations [25]. In the more realistic geometry of a cylin-

drical tube a similar problem was solved in Ref. [26]. It was obtained that the acceleration rate σ in cylindrical tubes is from 2 to 4 times larger (depending on Re) in comparison with the 2D case. So far the theory did not take into account heat losses to the walls and local flame quenching, which are inevitable in real experiments. Besides, the theory has to include turbulent burning like that observed in the DDT experiments [2–8]. All these effects influence, of course, the acceleration rate σ in Eq. (1), and they have to be taken into account in the theory of the flame acceleration. However, at present one may adopt acceleration of laminar flames in tubes with adiabatic walls as a physical model of the process, together with Eq. (2), which has been validated in direct numerical simulations [25]. It was demonstrated in Ref. [23] that such a model does capture the essence of the DDT mechanism.

In the present paper we study the next step in the DDT, namely, the compression wave pushed by an accelerating flame, and the explosion in the fuel mixture ahead of the flame front. We develop the analytical theory of the process within the approximation of a one-dimensional isentropic flow. The isentropic approximation is rigorous until a shock is formed in the compression wave. After that instant, the isentropic approximation may be considered only as a model, which is justified by the relatively small entropy jump in shocks of moderate intensity [1]. We find the condition of the explosion in the compression wave ahead of the flame front, and the time of the shock formation. If the explosion happens before the shock is formed, then the isentropic approach remains rigorous, which imposes limitations on the activation energy of the reaction. Beyond that limits the present theory may be treated as a model. We compare the developed theory to the results of direct numerical simulations on the DDT in a laminar flow [23]. We find good agreement between the analytical and numerical results and discuss the reasons of possible minor deviations.

II. INSTANT OF THE GAS EXPLOSION

We consider a flame front with the normal velocity U_f propagating in a tube of radius R from a closed end of the tube. In that case the accelerating flame is similar to a semitransparent piston, which moves in the laboratory reference frame with the velocity

$$U_l = \Theta U_w = \Theta U_f \exp\left(\sigma \frac{U_f t}{R}\right), \tag{3}$$

so that the position of such a piston is given by

$$X_l = R\frac{\Theta}{\sigma}\left[\exp\left(\sigma \frac{U_f t}{R}\right) - 1\right]. \tag{4}$$

At the same time, the velocity of the flow pushed by the flame is different from Eq. (3), it is equal to

$$U_p = (\Theta - 1) U_f \exp\left(\sigma \frac{U_f t}{R}\right) \tag{5}$$

just ahead of the flame front at $x = X_l$. As long as the flow is isentropic, the velocity u ahead of the flame is described indirectly by the equation [1]

$$x = t\left(c_0 + \frac{\gamma+1}{2}u\right) + F(u), \tag{6}$$

where c_0 is the initial sound speed, γ is the adiabatic exponent, and the function $F(u)$ has to be determined from the boundary conditions at the "piston." In the following we will work with the dimensionless variables $z = x/R$, $\tau = U_f t/R$, $w = u/U_f$, $Z_l = X_l/R$, $f = F/R$, $W_p = U_p/U_f$. Then Eqs. (3)–(6) may be rewritten as

$$W_l = \Theta \exp(\sigma\tau), \tag{7}$$

$$Z_l = \frac{\Theta}{\sigma}\left[\exp(\sigma\tau) - 1\right], \tag{8}$$

$$W_p = (\Theta - 1)\exp(\sigma\tau), \tag{9}$$

$$z = \tau\left(\mathrm{Ma}^{-1} + \frac{\gamma+1}{2}w\right) + f(w), \tag{10}$$

where $\mathrm{Ma} = U_f/c_0$ plays the role of the Mach number. We calculate the function $f(w)$ taking into account the boundary condition $w = W_p$ at the flame front $z = Z_l$,

$$f(W_p) = Z_l - \tau\left(\mathrm{Ma}^{-1} + \frac{\gamma+1}{2}W_p\right). \tag{11}$$

Substituting Eq. (9) into Eq. (8) we find

$$Z_l = \frac{\Theta}{\Theta - 1}\frac{W_p}{\sigma} - \frac{\Theta}{\sigma} = \frac{\Theta}{\Theta - 1}\frac{w}{\sigma} - \frac{\Theta}{\sigma}. \tag{12}$$

Taking into account time dependence of the velocity at the piston $w = W_p$, Eq. (9), or

$$\tau = \sigma^{-1}\ln\left(\frac{w}{\Theta - 1}\right), \tag{13}$$

we obtain the function $f(w)$ in Eq. (10),

$$f(w) = \frac{\Theta}{\Theta - 1}\frac{w}{\sigma} - \frac{1}{\sigma}\ln\left(\frac{w}{\Theta - 1}\right)\left(\mathrm{Ma}^{-1} + \frac{\gamma+1}{2}w\right) - \frac{\Theta}{\sigma}. \tag{14}$$

As a result, the velocity distribution $w = w(z, \tau)$ produced by an accelerating flame is determined indirectly by Eq. (10) with the function $f(w)$ specified by Eq. (14). Formulas (10), (14) work as long as the flow is isentropic, that is, as long as there is no shock in the flow. At this point one has to stress that even a stationary planar flame front propagating from a closed end of a tube generates a weak shock. Still, such a shock is ultimately weak, since a typical evaluation for the Mach number characterizing the flame is $\mathrm{Ma} = U_f/c_0 = 10^{-3}$. In the limit of $\mathrm{Ma} \ll 1$ the flow pushed by the planar flame may be described as a linear compression wave propagating with the speed of sound c_0, which does not change the entropy of the gas. A noticeably stronger shock may develop later in the flow, violating the isentropic approximation. In Sec. IV of the present paper we will find the instant of the shock formation, which indicates the rigorous limits of the

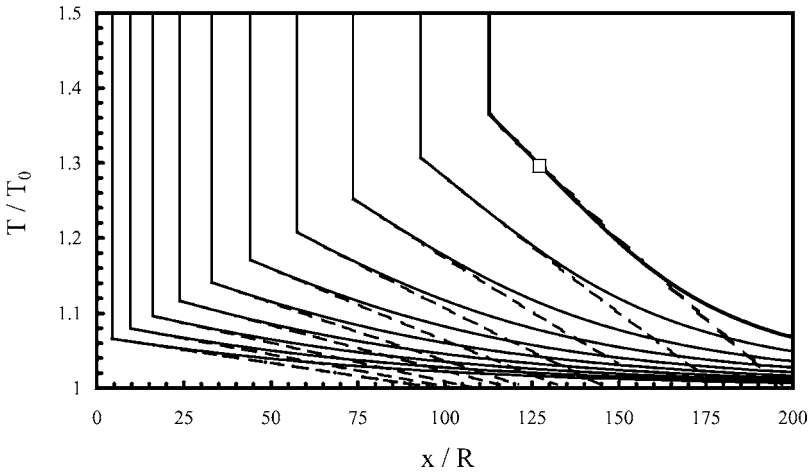

FIG. 1. Temperature profiles ahead of the flame front for $\Theta=5$ and $R/L_f=50$ at $tU_f/R=0.8-6.4$ with time intervals 0.8. The bold line corresponds to $tU_f/R=7.9$, when the system Eqs. (36), (37) is satisfied. The marker shows the respective position. The dashed lines present the temperature profiles calculated using Eq. (27).

isentropic approach. Meanwhile, we assume the velocity distribution (10), (14) valid with no limitations.

We are interested mainly in the temperature increase in the compression wave, since the reaction rate is strongly coupled to the temperature. For that purpose we calculate the local sound speed in the isentropic flow according to [1]

$$c = c_0 + \frac{\gamma-1}{2}u, \tag{15}$$

with the temperature increase

$$\frac{T}{T_0} = \left(\frac{c}{c_0}\right)^2 = \left(1 + \frac{\gamma-1}{2}\frac{u}{c_0}\right)^2. \tag{16}$$

In the dimensionless variables with $\vartheta=T/T_0$ the same formula is

$$\vartheta = \left(1 + \frac{\gamma-1}{2}w\,\mathrm{Ma}\right)^2. \tag{17}$$

As an illustration, the temperature distribution in a compression wave generated by a flame is shown in Fig. 1 for $\Theta=5$ and $R/L_f=50$, which corresponds to the acceleration rate $\sigma=0.23$ of Eq. (2). Other parameters $\mathrm{Ma}=0.045$, $\gamma=1.3$ are the same as in the simulations [23]. The temperature profiles are shown for the different time instants $U_f t/R=0.8-6.4$ with the interval 0.8; the last profile (selected by bold) corresponds to the time instant $U_f t/R=7.9$. The vertical lines indicate the temperature jump at the flame front.

An explosion happens if the reaction is completed in a gas element of the fuel mixture earlier than this element is burnt by the flame front. Suppose that the temperature of the gas element increases because of the heat release in the reaction only. Then such a gas element explodes abruptly after some preliminary time interval called the induction time τ_i, which depends on the gas temperature and on the chemical parameters, $\tau_i=\tau_i(T)$ [3]. Typically, the dependence $\tau_i=\tau_i(T)$ is extremely strong; therefore in order to find the condition for the explosion we have to study only the region of maximal temperatures just ahead of the flame front. In that case we are interested in the velocity distribution close to the flame in the form

$$w = W_p + \left(\frac{\partial w}{\partial z}\right)_{\tau,w=W_p}(z - Z_l). \tag{18}$$

Calculating the derivative from Eq. (10) we find

$$1 = \tau\frac{\gamma+1}{2}\left(\frac{\partial w}{\partial z}\right)_\tau + \left(\frac{df}{dw}\right)_{w=W_p}\left(\frac{\partial w}{\partial z}\right)_\tau, \tag{19}$$

or

$$\left(\frac{\partial w}{\partial z}\right)_\tau = \left[\tau\frac{\gamma+1}{2} + \left(\frac{df}{dw}\right)_{w=W_p}\right]^{-1}, \tag{20}$$

with

$$\frac{df}{dw} = \frac{\Theta}{(\Theta-1)\sigma} - \frac{\gamma+1}{2\sigma}\ln\left(\frac{w}{\Theta-1}\right) - \frac{1}{\sigma}\left(\frac{1}{w\,\mathrm{Ma}} + \frac{\gamma+1}{2}\right). \tag{21}$$

Respectively, for $w=W_p=(\Theta-1)\exp(\sigma\tau)$ we obtain

$$\frac{df}{dw} = \frac{\Theta}{(\Theta-1)\sigma} - \frac{\gamma+1}{2}\tau - \frac{1}{\sigma}\left(\frac{1}{W_p\mathrm{Ma}} + \frac{\gamma+1}{2}\right), \tag{22}$$

which leads to

$$\left(\frac{\partial w}{\partial z}\right)_\tau = \sigma\left(\frac{\Theta}{\Theta-1} - \frac{1}{\mathrm{Ma}W_p} - \frac{\gamma+1}{2}\right)^{-1}, \tag{23}$$

or

$$\left(\frac{\partial w}{\partial z}\right)_\zeta = -\frac{\sigma\zeta}{A(B-\zeta)}, \tag{24}$$

where a time-related variable $\zeta=\exp(\sigma\tau)$ is introduced together with the following designations:

$$A = \frac{\Theta}{\Theta-1} - \frac{\gamma+1}{2}, \tag{25}$$

$$B = \frac{1}{A(\Theta-1)\mathrm{Ma}}. \tag{26}$$

For the parameters $\Theta=5$, $\gamma=1.3$, $\mathrm{Ma}=0.045$ used in Ref. [23] we find $A=0.1$, $B=55.56$. According to Eq. (24), the

velocity distribution just ahead of the flame front takes the form

$$w = (\Theta - 1)\zeta - \frac{\sigma\zeta}{A(B-\zeta)}\left[z - Z_l(\zeta)\right], \tag{27}$$

with $Z_l = \Theta(\zeta - 1)/\sigma$. Approximating the velocity distribution ahead of the flame front by Eq. (27) we may calculate the respective temperature by using Eq. (17). The temperature profiles found in that way are presented in Fig. 1 by the dashed lines. As we can see, the linear approximation for the velocity profile, Eq. (27), works quite well in the vicinity of the flame front.

At this step, using the velocity distribution (27), we have to find the trajectories of the gas particles. The velocity of a gas particle is equal to

$$w \equiv \frac{dz}{d\tau} = \sigma\zeta\frac{dz}{d\zeta}. \tag{28}$$

Substituting Eq. (28) into Eq. (27) we obtain an equation for the trajectories of the gas particles close to the flame front,

$$\frac{dz}{d\zeta} = \frac{\Theta - 1}{\sigma} - \frac{z - Z_l}{A(B-\zeta)}, \tag{29}$$

with the solution

$$z(\zeta) - Z_l(\zeta) = C(B-\zeta)^{1/A} - \frac{A(B-\zeta)}{\sigma(1-A)}. \tag{30}$$

In principle, the integration constant C in Eq. (30) may be determined using the initial position of the gas particle z_0. However, as we will see below, the value z_0 is not important for the problem, and we leave the integration coefficient C as it is. A gas particle is consumed by the flame front at the time instant τ_c (corresponding to ζ_c) when

$$z(\zeta_c) = Z_l(\zeta_c). \tag{31}$$

Then, using Eq. (30) we can express the integration constant C by use of τ_c (or ζ_c),

$$C = \frac{A(B-\zeta_c)^{1-1/A}}{\sigma(1-A)}, \tag{32}$$

and Eq. (30) may be rewritten as

$$z(\zeta) - Z_l(\zeta) = \frac{A(B-\zeta)}{\sigma(1-A)}\left[\left(\frac{B-\zeta_c}{B-\zeta}\right)^{1-1/A} - 1\right], \tag{33}$$

which leads to

$$\zeta_c = B - (B-\zeta)\left(1 + \frac{\sigma(1-A)}{A(B-\zeta)}(z - Z_l)\right)^{-A/(1-A)}, \tag{34}$$

or

$$\zeta_c \equiv \exp(\sigma\tau_c) = B - (B-\zeta) \times\left[1 + \frac{\sigma(1-A)}{A(B-\zeta)}\left(z - \frac{\Theta}{\sigma}[\zeta - 1]\right)\right]^{-A/(1-A)}, \tag{35}$$

where we have substituted the expression for Z_l from Eq. (8). Thus we express the value ζ_c as a function of time ζ and the position z. That is, for every gas element at the point z at time τ (or ζ) we know the time instant when it will be consumed by the flame, $\tau_c = \sigma^{-1}\ln\zeta_c$. This value determines also the time interval $\tau_c - \tau$ left for a gas element before it will be burnt by the flame.

The gas element explodes definitely, if $\tau_c - \tau$ in the point z at time τ is larger than the induction time at the same point and time, $\tau_i = \tau_i[\vartheta(z,\tau)] = \tau_i(z,\tau)$ (in reality, it explodes even earlier, since temperature increases and the induction time decreases as the gas element comes closer to the flame front). Thus the sufficient condition of the explosion is given by the equation

$$\tau_i(z,\tau) + \tau - \tau_c(z,\tau) = 0, \tag{36}$$

which compares these two time intervals. If Eq. (36) is satisfied at a certain time instant τ' at least at one point z, then the respective gas element explodes ahead of the flame front. The explosion happens at the time instant $\tau' + \tau_i$, that is, the induction time later after the condition (36) is satisfied. As we can see from Eq. (36), the explosion happens at $\tau_c(\tau') = \tau' + \tau_i(\tau')$. Equation (36) contains two variables, τ and z, which formally implies a dependence $\tau' = \tau'(z)$. In order to find the explosion time, we are interested in the smallest possible τ' satisfying Eq. (36) for any z. To minimize τ' we obtain an additional equation from Eq. (36),

$$\left(\frac{\partial\tau_i}{\partial z}\right)_\tau = \left(\frac{\partial\tau_c}{\partial z}\right)_\tau. \tag{37}$$

The solution to the set of Eqs. (36), (37) determines τ' and the instant of the explosion $\tau_c(\tau')$.

III. INDUCTION TIME

The system (36), (37) contains two functions, $\tau_c(\tau,z)$ and $\tau_i = \tau_i[\vartheta(z,\tau)] = \tau_i(z,\tau)$. The first one, $\tau_c(\tau,z)$, was obtained in the previous section, see Eq. (35). In the present section we provide information on the other function, the induction time versus temperature of a gas particle. The induction time shows how long a time is needed for the reaction to be completed in a gas element. In paper [23] the reaction mechanism in the DDT was described by a single irreversible reaction of Arrhenius type. In reality, the induction time at low temperature (ahead of the flame front) is not controlled by the same Arrhenius law as that governing the heat release at high temperature (inside the flame). For hydrocarbon mixtures and for hydrogen-oxygen mixtures, the chemical reaction shows a crossover temperature, about 1000 K, below which the reaction rate slows down drastically (transition due to the competition between chain branching and chain breaking) [27]. This explains different combustion phenomena as, for example, the flammability limits; this is also important for the DDT. Due to these limitations, the temperature increase ahead of an accelerating laminar flame in experiments (taking into account thermal losses) is not sufficiently high to ignite a cold fuel mixture [27–29], and the DDT is observed only for turbulent flames [2–8]. However, with all these complications in mind, with rather moderate success in the theory of turbulent burning, one has little hope

to develop any theory of the DDT. To develop a theory, it is important to start at least with simple models, which provide basic quantitative description of the process, and which may be later elaborated into more realistic and much more complicated results. Therefore in the present paper we use the simplified model of the one-step irreversible Arrhenius reaction for the flame acceleration and the DDT as it was proposed and verified in Ref. [23]. In addition, we will use another simple and relevant model of an Arrhenius law with a cut off temperature. Investigation of more realistic reaction mechanisms is a large part of the combustion science, which is far beyond the scope of the present paper.

We start with a single irreversible reaction of Arrhenius type of the first order,

$$\frac{dY}{dt} = -\frac{Y}{t_R}\exp\left(-\frac{E}{R_g T}\right), \tag{38}$$

where Y is the concentration of the fresh fuel mixture, t_R is the reaction constant of time dimension, R_g is the ideal gas constant, and E is the activation energy, which is typically high, $E/R_g T \gg 1$. Particularly, a reaction like Eq. (38) was used in the direct numerical simulations of the DDT in a laminar flow [23]. Using the Arrhenius reaction as an example, we will demonstrate how one can calculate the time of the explosion ahead of an accelerating flame front. Study of the explosion triggering using more complicated chemical kinetics will be presented elsewhere. According to Ref. [3], a gas element explodes after the induction time,

$$t_i = t_R C_P \frac{R_g T^2}{EQ}\exp\left(\frac{E}{R_g T}\right), \tag{39}$$

where Q is the heat release in the reaction, and C_P is the respective heat capacity at constant pressure. Formula (39) requires additional explanations. It was derived assuming that a gas particle is "suddenly" put at an increased temperature at the initial time as, for example, when crossing a shock. In the case of a continuous compression wave investigated in Sec. II the initial temperature of a gas particle also increases, but the increase goes continuously. In that case Eq. (39) may be used only in the limit of high activation energy, $E/R_g T \gg 1$ (in fact, it was derived only for that limit). Then the development of the reaction at lower temperatures may be neglected in comparison with the reaction at higher temperatures, as long as the temperature increases because of an external reason like a compression wave. A similar situation takes place inside a flame front, where the temperature increases continuously due to thermal conduction from the initial value to the final one with negligible reaction. The whole reaction takes place in a tiny zone, where the temperature differs only slightly from the final value. In the compression wave the reaction also becomes important only when the temperature comes sufficiently close to the maximal value just ahead of the flame front [when the conditions (36), (37) are satisfied]. Then temperature of the gas element increases both due to the compression and the reaction, and the reaction process requires a shorter time than that determined by Eq. (39). We stress that our theory specifies sufficient conditions for the explosion and determines the explosion time from above. In the general case of different reaction mechanisms at low and high temperatures there is no straight correlation between the coefficients in Eq. (39) and the parameters of the flame front. However, when both mechanisms are described by the same formula (38), like it was adopted in Ref. [23], the induction time (39) may be related to the flame velocity and thickness, U_f and L_f. For illustration purposes, first we neglect variations of these parameters because of the temperature increase ahead of the flame front, assume Lewis number equal unity and a constant coefficient of thermal conduction κ. The temperature dependence of the planar flame velocity will be taken into account at the end of this section. Then using the Zeldovich-Frank-Kamenetski theory [3] we find

$$U_f^2 = \frac{2\kappa T_b T_0}{\rho_f C_P t_R (T_b - T_0)^2}\left(\frac{R_g T_b}{E}\right)^2 \exp\left(-\frac{E}{R_g T_b}\right), \tag{40}$$

$$L_f = \frac{\kappa}{\rho_f C_P U_f}, \tag{41}$$

where T_b is the temperature of the burnt matter,

$$T_b/T_0 = 1 + Q/(C_P T_0) = \Theta. \tag{42}$$

Particularly, one may reduce Eqs. (40)–(42) to

$$U_f = \frac{2L_f \Theta^3}{t_R(\Theta - 1)^2}\left(\frac{R_g T_0}{E}\right)^2 \exp\left(-\frac{E}{R_g \Theta T_0}\right), \tag{43}$$

and the induction time may be written in a similar way as

$$t_i = t_R \frac{R_g T^2}{E(\Theta - 1)T_0}\exp\left(\frac{E}{R_g T}\right). \tag{44}$$

Expressing t_R from Eq. (43) and substituting into the relation for the induction time (44) we obtain

$$t_i = 2\frac{L_f}{U_f}\left(\frac{\Theta R_g T_0}{(\Theta - 1)E}\right)^3 \frac{T^2}{T_0^2}\exp\left[\frac{E}{R_g T_0}\left(\frac{T_0}{T} - \frac{1}{\Theta}\right)\right]. \tag{45}$$

Using the scaled variables introduced above we can rewrite Eq. (45) as

$$\tau_i = 2\frac{L_f}{R}\frac{\Theta^3 \vartheta^2}{(\Theta - 1)^3 \beta^3}\exp\left(\frac{\beta}{\vartheta} - \frac{\beta}{\Theta}\right), \tag{46}$$

where $\beta = E/(R_g T_0)$ is the scaled activation energy. In the dimensionless formulation of the problem (36), (37), the scaled induction time τ_i depends on the scaled tube width R/L_f. The acceleration rate σ of the flame front given by Eq. (2) also depends on the scaled tube width R/L_f due to the relation

$$\mathrm{Re} = \frac{R}{\mathrm{Pr} L_f}, \tag{47}$$

where Pr is the Prandtl number. Therefore choosing a particular tube width R/L_f we specify both the acceleration rate and the induction time τ_i (with the other parameters fixed), and we may solve the problem (36), (37), that is, we may find the time τ' and the explosion instant $\tau_c(\tau')$. The formulated problem was solved numerically. Solution to Eq. (36) is

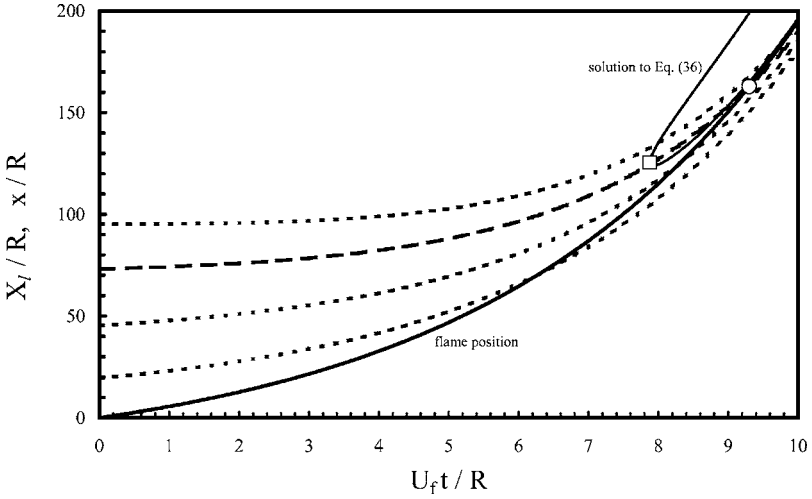

FIG. 2. Trajectories of the flame front (the bold solid line) and of gas particles ahead of the flame (the dotted and dashed lines) for $\Theta=5$ and $R/L_f=50$. The particles are consumed by the flame at the time instants $t_c U_f/R=6.3;8.3;9.3;9.8$. The line selected by large dashes corresponds to the particle, which may explode first just ahead of the flame front at $t_c U_f/R=9.3$. Solution to Eq. (36) is shown by the other solid line. The position of minimal time, satisfying Eq. (36), and the explosion position are shown by the square and circular markers, respectively.

illustrated in Fig. 2 for the parameters $\Theta=5$, $\gamma=1.3$, Ma $=0.045$ used in Ref. [23] and for the tube of radius $R/L_f=50$ with $\sigma=0.23$. The solid line presents the flame position versus time, while the dashed lines show trajectories of gas particles. The loop in Fig. 2 is the solution to Eq. (36). Gas particles inside the loop may explode ahead of the flame front. The square marker indicates the point at the loop corresponding to minimal time [the solution to Eqs. (36), (37)]. Trajectory of the respective particle is selected by larger dashes. The particle reaches the flame front at the time instant $\tau_c=9.3$ shown by circular marker. The explosion happens at this time and place. One more dotted line in Fig. 2 describes a particle, which would be consumed by the flame at the time instant $\tau_c=9.8$. Still, in the time interval $9.3<\tau<9.8$, such a trajectory is only hypothetic, since the explosion happens earlier. The solution to the problem (36), (37) is shown in Fig. 3 versus the scaled activation energy β for $\Theta=5$, $\gamma=1.3$, Ma$=0.045$ and different $R/L_f=20,50,100$, which correspond to $\sigma=0.53;0.23;0.12$, respectively. The locus of the explosion from Fig. 2 is shown by the marker. As we can see, the explosion time increases noticeably with the increase of the activation energy. Still, this dependence is not extremely dramatic like that given by Eq. (44) [or by Eq. (46) in the scaled form]. Particularly, taking $\beta=E/(R_g T_0)=20$ similar to paper [23] we obtain $\tau'=4.6;7.9;8.3$ and $\tau_c=5.0;9.3;14.9$ for $R/L_f=20,50,100$. In Fig. 1 the temperature profile corresponding to $\tau'=7.9$ is indicated by bold; the respective position, where the system (36), (37) is satisfied, is shown in Figs. 1 and 2 by the square marker.

It is also interesting to consider the model of an Arrhenius reaction with a cutoff temperature T_z. According to that model, the reaction rate is determined by Eq. (38) at $T>T_z$, and it is zero at $T<T_z$. Then the explosion time becomes sensitive to the cutoff. Solution to the set of Eqs. (36), (37) together with the Arrhenius law (39) determines the time τ' and the position $z'=z(\tau')$ of a gas particle, for which the Arrhenius reaction goes sufficiently fast to guarantee the explosion. The same equations [together with Eqs. (17), (27)] determine also the temperature of the gas element $T'=T(x',t')$ [or $\vartheta'=\vartheta(z',\tau')$ in the dimensionless units]. At that point one has to compare T' to the cut off temperature T_z. In the case of $T'>T_z$, the Arrhenius reaction is "permitted," and the explosion happens. In the opposite case of $T'<T_z$, the Arrhenius reaction is forbidden, and one has to wait longer for the explosion. Then the system of equations (36), (37) has to be modified: the equation (37) of minimal possible time must be replaced by the cutoff condition

$$\vartheta(z',\tau')>\vartheta_z. \tag{48}$$

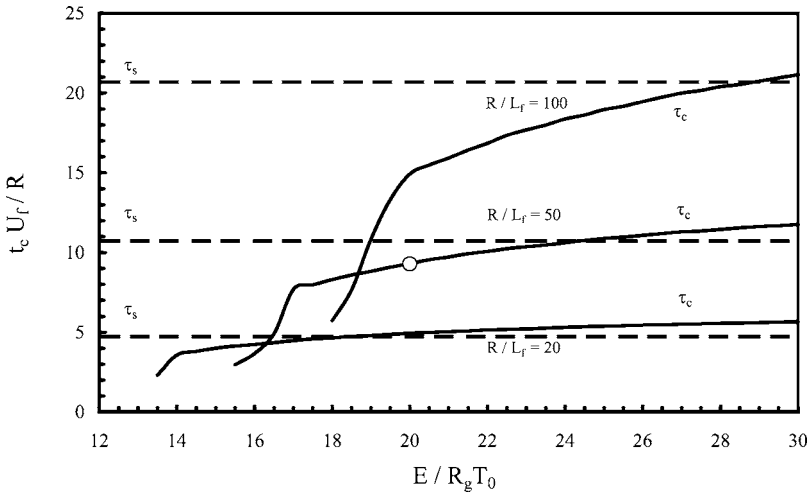

FIG. 3. The explosion time τ_c versus the scaled activation energy for $R/L_f=20;50;100$, (a), (b), (c), respectively. The dashed lines present the instant τ', when the system (36), (37) is satisfied. The dotted line shows the time of shock formation τ_s. The locus of explosion from Fig. 2 is shown by the marker.

For example, for the parameters $\Theta=5$, $\gamma=1.3$, Ma$=0.045$, $R/L_f=50$ considered above, the explosion is delayed in comparison with that of Fig. 1 if $\vartheta_z>1.3$. Evaluating the dimensional cutoff as 1000 K [27] we can see that the explosion proceeds according to the simple Arrhenius mechanism only for the initial temperature $T_0>770$ K. This corresponds to a noticeably preheated fuel mixture. However, the whole set of parameters of the simulations [23] resemble a flame with preliminary preheating.

In the case of the Arrhenius reaction with a cutoff temperature $\vartheta'<\vartheta_z$, the explosion time may be also found in another way. When the condition (36) is satisfied, the temperature just ahead of the flame differs slightly from the temperature ϑ', with the evaluation

$$\vartheta(Z_l)-\vartheta'=O(\beta^{-1}) \tag{49}$$

for $\beta\gg1$. Then the explosion time may be evaluated from above by the condition that temperature just ahead of the flame is equal to the cutoff temperature

$$\vartheta(Z_l)=\vartheta_z. \tag{50}$$

Taking into account Eqs. (17) and (19) we find

$$\vartheta_z=\left(1+\frac{\gamma-1}{2}\mathrm{Ma}(\Theta-1)\exp(\sigma\tau_c)\right)^2, \tag{51}$$

which leads to the explosion time

$$\tau_c=\sigma^{-1}\ln\left(2\frac{\vartheta_z^{1/2}-1}{\mathrm{Ma}(\gamma-1)(\Theta-1)}\right). \tag{52}$$

According to Eq. (52), in that case the explosion time is indeed strongly sensitive to the temperature cutoff.

We have to stress also that in our theory the explosion happens just ahead of the flame front. Still, the experiments [30] demonstrate two possibilities. In some cases the explosion happens at the flame front in agreement with the present theory. In other cases the explosion is observed noticeably ahead of the flame front, and it is preceded by the formation of a strong shock in the compression wave. Obviously, the theory is relevant only to the first type of the DDT, while the second one is beyond the present analysis. Still, even in the first case the present theory cannot be applied straightforward to analyze the experiments. All experiments [30] demonstrate the shock formation before the explosion triggering. Strictly speaking, a shock violates the condition of an isentropic flow used in the present paper. However, sometimes shock influence may be minor even quantitatively, as we show below in Sec. V.

There is one more effect of the model, which requires a discussion. To obtain the solution of Fig. 3 we assumed that the planar flame velocity U_f is constant in the acceleration process. In reality, it varies in time because of the temperature variations just ahead of the flame front, see Eqs. (17), (40). The increase of U_f may be taken into account, for example, as corrections to the acceleration rate Eq. (2). We point out that the theory of Sec. II was developed independent of any particular value for the acceleration rate. The acceleration rate comes into the theory as an external information. Equation (2) determines the acceleration rate in a 2D laminar flow produced by a flame in a tube with adiabatic walls. Taking into account turbulence and thermal losses to the walls, one will come to a modified expression for σ. Another modification happens because of the temperature dependence of U_f. Particularly, for the parameters $\Theta=5$, $\gamma=1.3$, Ma$=0.045$, and $R/L_f=50$ used in Fig. 1 the modified acceleration rate may be estimated as $\sigma_m=0.27$ instead of $\sigma=0.23$ considered above. As we can see, the increase of the planar flame velocity provides minor corrections to the acceleration rate, about 17%. Increase of the acceleration rate modifies also the time instant of the explosion: we obtain $\tau_c=8.05$ instead of $\tau_c=9.3$ demonstrated in Figs. 1–3.

IV. LIMITATIONS OF THE THEORY DUE TO THE SHOCK FORMATION

The analytical theory developed above is based on the assumption of an isentropic flow ahead of the flame front. The assumption holds until a shock develops inside the compression wave. As the flame accelerates, the compression wave becomes stronger because of the nonlinear structure of Eqs. (10), (14), which eventually produces a relatively strong shock wave. A shock wave arises, when the function $w=w(z,\tau)$ becomes multiple valued, that is, when bending appears in the function $z=z(w,\tau)$

$$\left(\frac{\partial z}{\partial w}\right)_\tau=0, \quad \left(\frac{\partial^2 z}{\partial w^2}\right)_\tau=0. \tag{53}$$

The above equations applied to Eq. (10) determine the time τ_s and the position z_s of the shock formation, and the flow velocity at the arising shock w_s [1],

$$\frac{\gamma+1}{2}\tau_s=-\left(\frac{df}{dw}\right)_{w=w_s}, \quad \left(\frac{d^2 f}{dw^2}\right)_{w=w_s}=0. \tag{54}$$

Taking into account Eq. (14) we calculate

$$\frac{df}{dw}=\frac{\Theta}{(\Theta-1)\sigma}-\frac{\gamma+1}{2\sigma}\ln\left(\frac{w}{\Theta-1}\right)-\frac{1}{\sigma w}\left(\frac{1}{\mathrm{Ma}}+\frac{\gamma+1}{2}w\right), \tag{55}$$

$$\frac{d^2 f}{dw^2}=-\frac{\gamma+1}{2\sigma w}+\frac{1}{\sigma\,\mathrm{Ma}w^2}. \tag{56}$$

Thus at the time and place of the shock formation the flow velocity is

$$w_s=\frac{2}{(\gamma+1)\mathrm{Ma}}, \tag{57}$$

which corresponds to

$$u_s=\frac{2c_0}{\gamma+1} \tag{58}$$

in the dimensional variables, and which is slightly below c_0. The time of the shock formation is calculated from Eq. (54) as

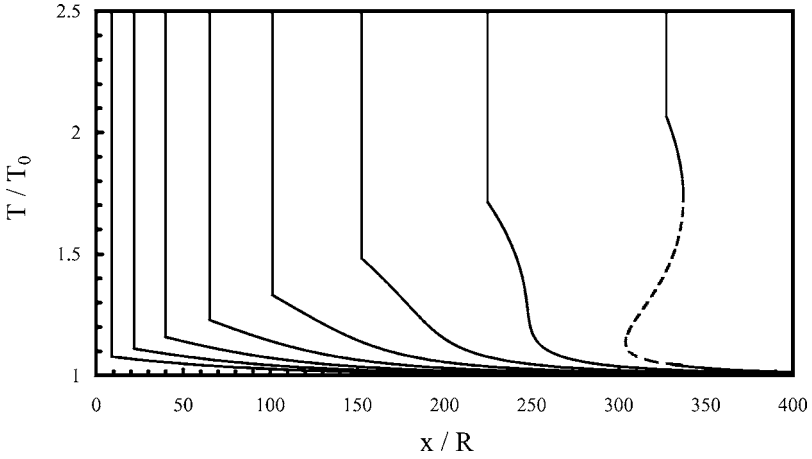

FIG. 4. Temperature profiles ahead of the flame front for $\Theta=5$ and $R/L_f=50$ at $tU_f/R=1.5-12$ with time intervals 1.5. The dashed line shows the multiple-valued part of the dependence.

$$\sigma\tau_s = -\frac{2\Theta}{(\gamma+1)(\Theta-1)} + 2 - \ln\left(\frac{\gamma+1}{2}(\Theta-1)\mathrm{Ma}\right). \tag{59}$$

In the approximation of $\mathrm{Ma}\to 0$ we obtain a simplified formula

$$\tau_s = -\frac{1}{\sigma}\ln\left(\frac{\gamma+1}{2}(\Theta-1)\mathrm{Ma}\right). \tag{60}$$

We can observe a shock formation in Fig. 4, which presents the temperature profiles for the same flow parameters as Fig. 1, but for a noticeably longer time period $tU_f/R=1.5-12$ with step 1.5. One can see a shock formation in the last but one temperature profile; the last profile corresponds formally to a multiple-valued function for the temperature. Using τ_s and w_s we find the position of the shock formation z_s from Eq. (10),

$$z_s = \frac{2}{\mathrm{Ma}}\tau_s + \frac{2\Theta}{\mathrm{Ma}(\Theta-1)(\gamma+1)\sigma} + \frac{2}{\mathrm{Ma}\,\sigma}\ln\left(\frac{\gamma+1}{2}(\Theta-1)\mathrm{Ma}\right) - \frac{\Theta}{\sigma}, \tag{61}$$

or

$$z_s = \frac{2}{\mathrm{Ma}\,\sigma}\left(2 - \frac{\Theta}{(\Theta-1)(\gamma+1)}\right) - \frac{\Theta}{\sigma}. \tag{62}$$

We find also the temperature at the point z_s,

$$\frac{T_s}{T_0} = \vartheta_s = \left(1+\frac{\gamma-1}{\gamma+1}\right)^2 = \frac{4\gamma^2}{(\gamma+1)^2}. \tag{63}$$

The time of the shock formation determines the validity limits of the present theory. In the case of $\Theta=5$ and $R/L_f=20;50;100$ (with $\sigma=0.53;0.23;0.12$) the time instants of the shock formation τ_s are presented in Fig. 3 by the dotted horizontal lines. Intersections of these lines with the curves $\tau'=\tau'(E/R_gT_0)$ limit the domain of the activation energies, for which the present theory works rigorously. Still, even beyond that limits the theory may work rather well. Even after the shock formation, the intensity of the shock measured by the relative pressure jump remains moderate for some time. On the other hand, it is known that the entropy jump in a weak shock scales as cube of the pressure jump [1]. Because of the last fact, the isentropic approximation for the compression wave may work well even for some time after the shock formation.

V. COMPARISON TO THE NUMERICAL SIMULATIONS

It would be interesting to compare the present theory to the experiments. For that purpose one needs, first of all, an information about the acceleration rate of the flame front σ. Unfortunately, the experimental measurements did not address σ so far and they deal with turbulent burning. The experimental results concern typically the dimensional characteristic length or time of the DDT [4–8]. These values depend on σ, but they also involve the turbulent flame speed, which by itself is an important problem of hydrodynamics and combustion science waiting for solution. They also depend on the mechanism of chemical kinetics, which may be quite complicated in reality. By all these reasons, instead of real experiments, one can compare the theory to the numerical simulations.

To the best of our knowledge, so far there has been only one work on direct numerical simulations of the DDT in a laminar flow, which included all processes starting from the flame acceleration and up to the detonation wave [23]. We would like to stress that, though the idea of a laminar DDT allowed the possibility of direct numerical simulations of the process, still the task undertaken by Kagan and Sivashinsky in Ref. [23] remains extremely difficult from the numerical point of view. Indeed, when modeling the DDT one has to resolve the internal flame structure, the strongly curved shape of the accelerating flame front, the structure of the compression wave ahead of the front, and finally, the detonation structure. All these phenomena are characterized by quite different length and time scales. Therefore, trying to model all these processes in one simulation run in a reasonable time, a researcher inevitably faces considerable problems with the computational accuracy. As a result, one should expect much lower accuracy in Ref. [23], which studied the whole process of the DDT, in comparison with the papers [24,25], devoted to the flame acceleration only. Because of the accuracy limitations, the results of Ref. [23]

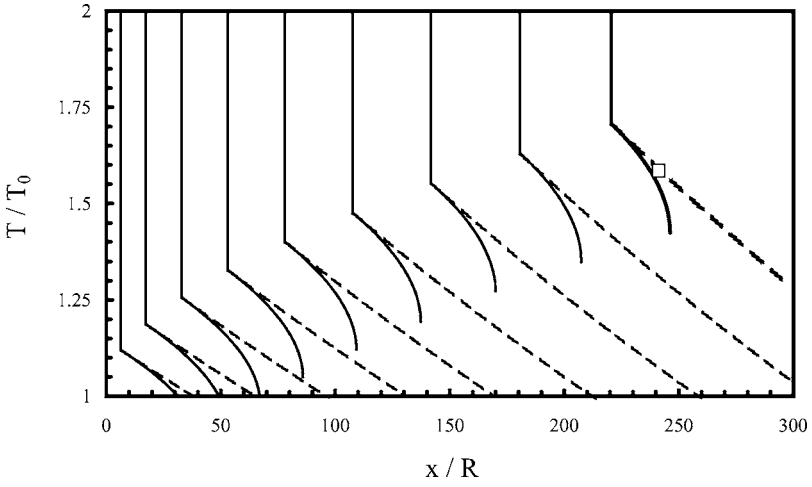

FIG. 5. Temperature profiles ahead of the flame front for $\Theta=5$ and $R/L_f=50$ for the acceleration regime Eq. (65) at $tU_f/R=0.8-6.4$ with time intervals 0.8. The bold line corresponds to $tU_f/R=7.14$, when the system Eqs. (36), (37) is satisfied. The marker shows the respective position. The dashed lines present the temperature profiles calculated using Eq. (68).

agree with Refs. [24,25] only qualitatively, but not quantitatively. Particularly, instead of the exponential regime of the flame acceleration, Eq. (1), observed in Refs. [24,25], paper [23] presented linear growth of the flame velocity with time,

$$W_l = \Theta W_w = \Theta(1 + a\tau), \tag{64}$$

with $a \approx 1.45$ for $R/L_f=5$. Therefore, in order to compare the present theory to the simulations [23], we have to perform additional calculations modifying the theory for the acceleration regime (64) instead of Eq. (1) considered in Sec. II. Then the flame position is calculated as

$$Z_l = \Theta\tau(1 + a\tau/2), \tag{65}$$

and the dimensionless velocity w ahead of the flame front is described indirectly by

$$z = \tau\left(\mathrm{Ma}^{-1} + \frac{\gamma+1}{2}w\right) + f(w), \tag{66}$$

with the function

$$f(w) = \frac{1}{2a}\left(1 - \frac{w}{\Theta - 1}\right)\left[2\,\mathrm{Ma}^{-1} - \Theta + \left(\gamma - \frac{1}{\Theta - 1}\right)w\right]. \tag{67}$$

The velocity distribution ahead of the flame front may be presented as

$$w(z,\tau) = (\Theta - 1)(1 + a\tau) + \frac{z - Z_l(\tau)}{p\tau - q}, \tag{68}$$

where we have introduced the coefficients

$$p = \frac{1}{\Theta - 1} - \frac{\gamma - 1}{2}, \tag{69}$$

$$q = \frac{1}{a}\left(\frac{\mathrm{Ma}^{-1} - 1}{\Theta - 1} + \frac{\gamma - 1}{2}\right). \tag{70}$$

To perform the comparison we used the parameters of the numerical study [23]: the expansion coefficient $\Theta=5$, the Mach number $\mathrm{Ma}=0.045$, and $\gamma=1.3$, which leads to the factors $p=0.1$ and $q=3.76$. The temperature in the compression wave is calculated by the same formula (17) as before. The temperature profiles for the acceleration regime (64) are presented by the solid lines in Fig. 5 for the different time

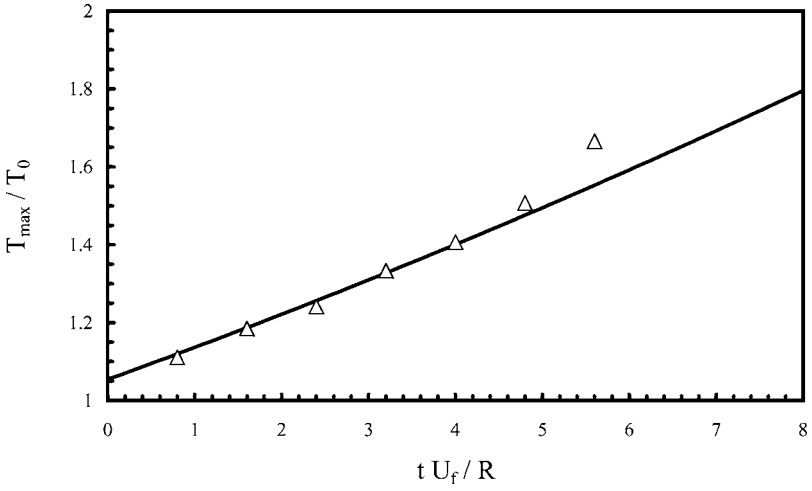

FIG. 6. Maximal temperature ahead of the flame front versus time according to the theory (solid line) and the simulations [23] (markers).

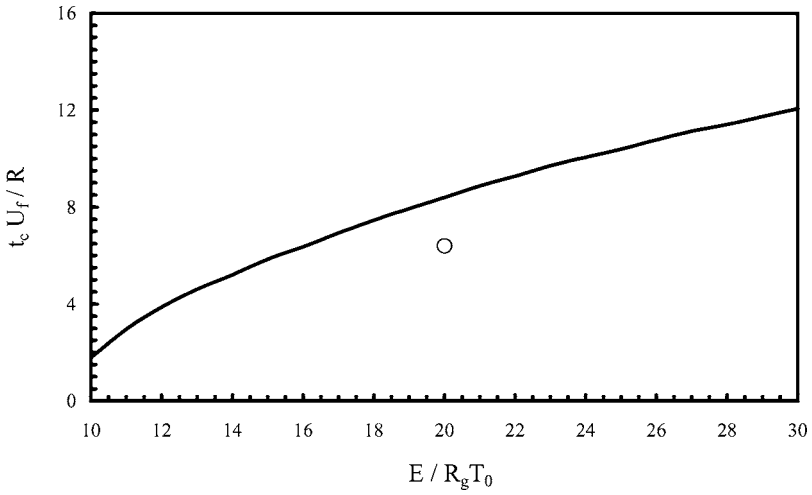

FIG. 7. The explosion time for the acceleration regime Eq. (65) versus the scaled activation energy according to the theory (solid line) and the simulations [23] (marker).

instants $\tau=tU_f/R=0.8-6.4$ with the time interval 0.8. The final profile shown by bold corresponds to the time instant $tU_f/R=7.14$, when the system (36), (37) is satisfied. Figure 6 shows the maximal temperature in the compression wave (just ahead of the flame front) versus time: the solid line presents the theoretical result Eqs. (17), (68); the markers correspond to the numerical simulations [23]. As we can see, the theory predicts the maximal temperature quite well; only at the time $tU_f/R=5.6$ the theoretical results underestimate the temperature a little, approximately by 6%.

To calculate the trajectories of the gas particles close to the flame front we rewrite Eq. (29) in the form

$$\frac{dz}{d\tau}=(\Theta-1)(1+a\tau)+\frac{z-Z_l(\tau)}{p\tau-q}, \tag{71}$$

with the solution

$$z=Z_l+\frac{a}{p(1-2p)}\zeta^2-\frac{p+aq}{p(1-p)}\zeta+C\zeta^{1/p}, \tag{72}$$

where a time-related variable $\zeta=1-p\tau/q$ is introduced for simplicity. A gas particle (at the position z at time τ) is consumed by the flame at the time instant $\tau_c=\tau_c(z,\tau)$. Respectively, taking $z(\tau_c)=Z_l(\tau_c)$ [or $z(\zeta_c)=Z_l(\zeta_c)$ for ζ variable], we rewrite Eq. (72) for $\zeta=\zeta_c$ in the form

$$\frac{a}{p(1-2p)}\zeta_c^{2-1/p}-\frac{p+aq}{p(1-p)}\zeta_c^{1-1/p}+C=0. \tag{73}$$

Substituting the constant C from Eq. (73) into Eq. (72) we find

$$z-Z_l(\zeta)+\frac{p+aq}{p(1-p)}\left[\zeta-\zeta_c\left(\frac{\zeta}{\zeta_c}\right)^{1/p}\right]-\frac{a}{p(1-2p)}\left[\zeta^2-\zeta_c^2\left(\frac{\zeta}{\zeta_c}\right)^{1/p}\right]=0. \tag{74}$$

Equation (74) determines an implicit dependence $\zeta_c=\zeta_c(\zeta,z)$, or $\tau_c=\tau_c(\zeta,z)$. Then, in order to find the explosion time, we have to solve the system (36), (37) with the function $\zeta_c=\zeta_c(\zeta,z)$ specified by Eq. (74) instead of Eq. (35). Solving the system numerically with the scaled activation energy $E/R_gT_0=20$ used in Ref. [23] we find the explosion time $\tau_c=8.4$. The last value exceeds a little the result $\tau_c=6.5$ obtained in Ref. [23]. The deviation of the results may be explained by the following reasons.

First of all, the numerical simulations [23] are two-dimensional (2D), while the present theory is only one-dimensional (1D). In a 2D geometry the curved flame shape leads to a multidimensional shock structure, collisions of the shocks may produce the so-called "hot points," which are impossible in the present 1D theory. It is generally accepted that the "hot points" reduce the explosion time, though up to now there was no quantitative answer to the question of how strong this reduction is. The real structure of the accelerating flame front is also curved and elongated, as it was obtained in Ref. [25], and not planar, as it is assumed in the 1D theory. The approximation of a planar piston becomes possible only when comparing the length scale of the flame front to the characteristic length scale of the compression wave with the factor proportional to Ma^{-1}. However, when we consider the process of explosion from the point of view of the curved flame front, then the explosion is expected to occur in the tongues of engulfed fresh mixture.

Second, the present theory holds rigorously until a shock is formed in the compression wave; after that the theory may work only as a model. However, for the simulation parameters of Ref. [23] the explosion happens after the shock formation, as we can see, for example, in Fig. 5. In that case, strictly speaking, the present theory may provide only evaluations. The relatively good agreement of the theory and the numerical simulations may be explained by the weak shock intensity (with the relative temperature jump about 0.5), which violates only slightly the assumption of an isentropic flow.

Finally, the deviations of the theory and the numerical simulations may be explained by the limited numerical accuracy of the simulations. To illustrate this, we have plotted the explosion time for the acceleration regime of Ref. [23] versus the scaled activation energy in Fig. 7; the explosion time obtained in the numerical simulations [23] is shown by the marker. As we can see, variations of the activation energy by 20% (from $E/R_gT_0=20$ to 16) modify the explosion time from $\tau_c=8.4$ found in the theory to $\tau_c=6.4$ observed in the

simulations. Still, such a variation of the activation energy is equivalent to a numerical error in calculating the temperature in the compression wave by 20%. The error of 20% would be quite normal for such a difficult numerical problem as that considered in Ref. [23]. By all these reasons, we can state that the present theory agrees well with the simulation results [23].

VI. SUMMARY

In the present paper we have developed the theory of explosion triggering by an accelerating flame in a tube. The theory describes the structure of the one-dimensional isentropic compression wave pushed by the flame front. The condition of explosion in the gas mixture ahead of the flame front is derived, Eqs. (36), (37), with the instant of the explosion τ_c determined by Eq. (35). In the dimensional variables, a gas element in the position x at time t may explode ahead of the flame front (after the induction time t_i), if the following system is satisfied:

$$t_i(T) + t - t_c(t,x) = 0, \tag{75}$$

$$\left(\frac{\partial t_i}{\partial x}\right)_t = \left(\frac{\partial t_c}{\partial x}\right)_t, \tag{76}$$

with the instant of explosion t_c calculated from

$$\exp(\sigma U_f t_c/R) = B - (B-\zeta) \times \left[1 + \frac{\sigma(1-A)}{A(B-\zeta)}\left(\frac{x}{R} - \frac{\Theta}{\sigma}[\zeta - 1]\right)\right]^{-A/(1-A)}, \tag{77}$$

where $\zeta = \exp(\sigma U_f t/R)$, and the constants A and B are defined by Eqs. (25), (26). The induction time $t_i(T)$ in Eqs. (75), (76) depends on temperature in the compression wave ahead of the flame front, which varies in time and space as

$$\frac{T}{T_0} = \left[1 + \frac{\gamma-1}{2}\,\mathrm{Ma}\,\zeta\left(\Theta - 1 - \frac{\sigma x/R - \Theta\zeta + \Theta}{A(B-\zeta)}\right)\right]^2. \tag{78}$$

Still, one has to specify the dependence $t_i = t_i(T)$ for any particular mechanism of chemical kinetics. In the present paper we demonstrate how the problem is solved in the case of a single reaction of Arrhenius type, controlling combustion both inside the flame front and ahead of the flame. We also considered the model of an Arrhenius reaction with a cutoff temperature, see Eq. (52). We find limitations of the theory due to the effect of the shock formation in the compression wave. We compare the theoretical results to the previous numerical simulations and find good agreement.

ACKNOWLEDGMENTS

The work was supported by the Swedish Research Foundation and by the Kempe Foundation. We thank Mikhail Ivanov for useful discussions.

[1] L. D. Landau and E. M. Lifshitz, *Fluid Mechanics* (Pergamon Press, Oxford, 1989).
[2] F. A. Williams, *Combustion Theory* (Benjamin, Menlo Park, CA, 1985).
[3] Ya. B. Zeldovich, G. I. Barenblatt, V. B. Librovich, and G. M. Makhviladze, *Mathematical Theory of Combustion and Explosion* (Consultants Bureau, New York, 1985).
[4] G. Roy, S. Frolov, A. Borisov, and D. Netzer, Prog. Energy Combust. Sci. **30**, 545 (2004).
[5] K. I. Shelkin, Zh. Eksp. Teor. Fiz. **10**, 823 (1940).
[6] J. E. Shepherd and J. H. S. Lee, in *Major Research Topics in Combustion* (Springer-Verlag, Hampton, VA, 1992), p. 439.
[7] S. Kerampran, D. Desbordes, and B. Veyssiere, Combust. Sci. Technol. **158**, 71 (2000).
[8] V. E. Tangirala, A. J. Dean, D. M. Chapin, P. F. Pinard, and B. Varatharajan, Combust. Sci. Technol. **176**, 1779 (2004).
[9] P. Clavin and F. A. Williams, J. Fluid Mech. **90**, 589 (1979).
[10] P. Searby and P. Clavin, Combust. Sci. Technol. **46**, 167 (1986).
[11] A. R. Kerstein, W. T. Ashurst, and F. A. Williams, Phys. Rev. A **37**, 2728 (1988).
[12] R. G. Abdel-Gayed, D. Bradley, and M. Lawes, Proc. R. Soc. London, Ser. A **414**, 389 (1987).
[13] R. C. Aldredge and F. A. Williams, J. Fluid Mech. **228**, 487 (1991).
[14] A. Pocheau, Phys. Rev. E **49**, 1109 (1994).
[15] R. C. Aldredge, V. Vaezi, and P. D. Ronney, Combust. Flame **115**, 395 (1998).
[16] B. Denet, Phys. Rev. E **59**, 2966 (1999).
[17] L. Kagan and G. Sivashinsky, Combust. Flame **120**, 222 (2000).
[18] B. Denet, Combust. Theory Modell. **5**, 85 (2001).
[19] D. Veynante and L. Vervisch, Prog. Energy Combust. Sci. **28**, 193 (2002).
[20] T. Lee and S. Lee, Combust. Flame **132**, 492 (2003).
[21] V. Bychkov, Phys. Rev. E **68**, 066304 (2003).
[22] V. Akkerman and V. Bychkov, Combust. Theory Modell. **9**, 323 (2005).
[23] L. Kagan and G. Sivashinsky, Combust. Flame **134**, 389 (2003).
[24] J. D. Ott, E. S. Oran, and J. D. Anderson, AIAA J. 41, 1391 (2003).
[25] V. Bychkov, A. Petchenko, V. Akkerman, and L.-E. Eriksson, Phys. Rev. E **72**, 046307 (2005).
[26] V. Akkerman, V. Bychkov, A. Petchenko, and L.-E. Eriksson, Combust. Flame **145**, 206 (2006).
[27] J. F. Griffiths and J. A. Barnard, *Flame and Combustion* (Blackie, London, 1995).
[28] P. F. Pinard, A. J. Higgins, and J. H. S. Lee, Combust. Flame **136**, 146 (2004).
[29] J. H. S. Lee, Annu. Rev. Phys. Chem. **28**, 75 (1977).
[30] P. A. Urtiev and A. K. Oppenheim, Proc. R. Soc. London, Ser. A **295**, 13 (1966).